The 2010 IEEE/RSJ International Conference on
Intelligent Robots and Systems
October 18-22, 2010, Taipei, Taiwan

Development of a hybrid control for a pneumatic teleoperation system using on/off solenoid valves

M.Q. Le, M.T. Pham, M. Tavakoli, R. Moreau

Abstract— **This paper presents a new predictive hybrid control law for a pneumatic teleoperation system using solenoid valves. Based on a predictive model of the mass flow rate of the valves, this method is used within a four-channel (4CH) bilateral control architecture for haptic teleoperation. An analysis of the controller parameters is carried out in order to achieve acceptable performances. The results show that a good accuracy in position and force tracking of the teleoperation system is obtained.**

Index terms—**Pneumatic actuators, on/off solenoid valve, hybrid control, teleoperation, bilateral control, transparency.**

I. Introduction

From its early use in the remote manipulation of radioactive materials, the application of teleoperation has expanded to include manipulation at different scales and in virtual worlds [1-4]. Teleoperation systems have the potential to play an important role in future remote or hazardous operations such as space and undersea explorations, forestry and mining, and also delicate operations such as micro-surgery and micro-assembly.

In a teleoperation system, a *slave* manipulator tracks the motion of a *master* manipulator, which is driven by a human operator. To improve the task performance, information about the environment is needed. Feedback about the environment can be provided to the human operator in many forms including audio, visual, or tactile information. Force feedback from the slave side to the master side, representing slave/environment contact information, provides a highly intuitive and natural sensation for the human operator [5]. When the contact force is reflected via the master actuator to the operator's hand, the teleoperation system is said to be bilateral.

In a bilateral teleoperation system, apart from the basic requirement of stability, there are primarily two design goals that ensure a close coupling between the human operator and the environment. The first goal is that the slave manipulator tracks the position of the master manipulator, and the second goal is that the environmental force acting on the slave, when a contact with the environment occurs, is accurately transmitted to the master [6]. Such a bilateral control allows to ensure the transparency of the teleoperation system.

M.Q. LE, M.T. Pham, and R. Moreau are with the Laboratoire Ampère, UMR CNRS 5005, Université de Lyon, INSA-Lyon, F-69621 Villeurbanne Cedex, France (corresponding author's e-mail: minh-quyen.le@ insa-lyon.fr). M. Tavakoli is with the Department of Electrical and Computer Engineering, University of Alberta, Canada, and currently on a research visit at INSA-Lyon.

In this study, we investigate the possibility to use electro-pneumatic systems as actuators in a teleoperation system. Pneumatic systems have recently become more popular due to their advantages of high mass-to-force ratio, being inert to magnetic fields, and recent breakthroughs in valve technology. Therefore, they have found use in new applications such as tele-robotics over the last few years [7], [8]. Two types of valves are generally used to control pneumatic systems: proportional servovalves and solenoid valves ("on/off valves"). Proportional servovalves have been successfully used to achieve high performances in various position or/and force control systems with pneumatic actuators, but they are usually expensive as they require high-precision manufacturing. In this paper, fast-switching on/off valves were chosen due to their low cost and small size. One of our objectives is to show that a good transparency in bilateral control can be obtained with these cheap components. The traditional method for controlling systems with solenoid valves is to use Pulse Width Modulation (PWM) to control the output mass flow rate of the valve [9], [10]. A main disadvantage of the PWM control is the chattering phenomenon due to the high frequency switching of the valve in steady state [11]. To overcome the PWM's disadvantages, this paper presents a new control method, which is based on the hybrid control theory recently developed by Retif *et al.* [12]. For this strategy, a predictive approach has been developed to determine the best control vector at each sample time to track the reference state [13]. In this paper, the hybrid control algorithm is applied for the force and position tracking in a 4CH bilateral teleoperation architecture. An analysis of the controller parameters is carried out in order to achieve an acceptable performance in terms of teleoperation system transparency.

Without loss of generality and for the sake of simplicity, the master and slave actuators are supposed to be identical in this study. The master and slave are one degree of freedom pneumatic manipulators. It should be noted that this paper does not deal with the presence of time delay in the teleoperation system's communication channel.

The structure of this paper is as follows. First, the modeling of the pneumatic manipulator composed of a cylinder and four solenoid valves is presented in Section II. Section III describes the design of a 4CH bilateral control architecture and provides the transparency conditions. Section IV presents experimental results that validate the proposed theories. Finally, concluding remarks appear in Section V.

II. MODEL OF THE PNEUMATIC SYSTEM

As mentioned above, the master and the slave manipulators are identical, thus only one pneumatic robot model is presented in this section. A schematic of a single degree of freedom pneumatic actuation system is shown in Fig. 1. The double-acting cylinder has equal areas on either side of the piston. To describe the cylinder's air flow dynamics, we assume that

- Air is a perfect gas,
- The pressure and the temperature are homogeneous in each chamber,
- The temperature variation in chambers is negligible - The mass flow rate leakages are negligible,
- The supply and exhaust pressures are constant.

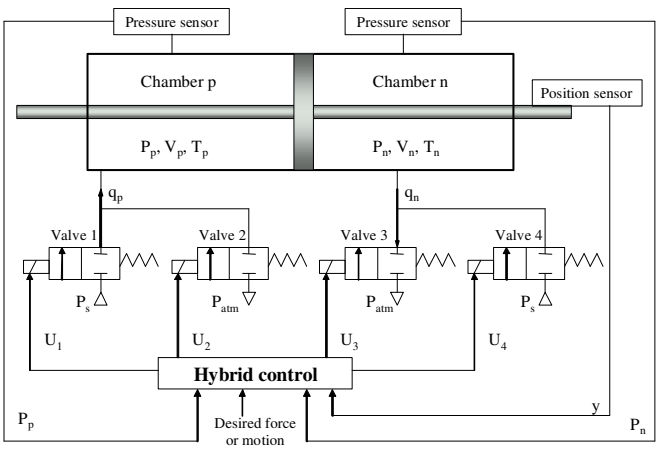

Fig. 1. Electro-pneumatic force control system with four valves

A. Model of the pneumatic chambers

The behavior of the pressure inside each chamber of the cylinder can be expressed as [14]

$$\begin{cases} \dfrac{dP_p}{dt} = \dfrac{\gamma r T_a}{V_p(y)}\left(q_p(U_1,U_2,P_p) - \dfrac{P_p}{rT_a}Sv\right) \\ \dfrac{dP_n}{dt} = \dfrac{\gamma r T_a}{V_n(y)}\left(q_n(U_3,U_4,P_n) + \dfrac{P_n}{rT_a}Sv\right) \end{cases} \quad (1)$$

where U_1, U_2, U_3 and U_4 are the control voltages of valve 1, valve 2, valve 3, and valve 4; y and v are the position (m) and velocity (m/s) of the piston; P_p and P_n are the pressures inside chambers p and n (Pa); V_p and V_n are the volumes of chambers p and n (m^3); S is the piston cylinder area (m^2); q_p and q_n are the mass flow rates in chambers p and n (kg/s); T_a is the temperature of the supply air (K); r is the perfect gas constant (J/(kg.K)) and γ is the polytropic constant.

B. Model of the valves

The mass flow rate characteristics of the on/off valves can be expressed as a function of the discrete control voltages and the pressures:

$$q_p(U_1,U_2,P_p) = \begin{cases} q_m(P_s,P_p) & \text{for } U_1=1 \text{ and } U_2=0 \\ 0 & \text{for } U_1=0 \text{ and } U_2=0 \\ -q_m(P_p,P_{atm}) & \text{for } U_1=0 \text{ and } U_2=1 \end{cases} \quad (2)$$

$$q_n(U_3,U_4,P_n) = \begin{cases} -q_m(P_s,P_n) & \text{for } U_3=1 \text{ and } U_4=0 \\ 0 & \text{for } U_3=0 \text{ and } U_4=0 \\ q_m(P_n,P_{atm}) & \text{for } U_3=0 \text{ and } U_4=1 \end{cases} \quad (3)$$

where P_s and P_{atm} are the pressures of the supply air and atmosphere. The '0' value of the input voltage corresponds to closed valve and the '1' value corresponds to open valve. All the states where $U_1 = U_2 = 1$ and $U_3 = U_4 = 1$ are prohibited to avoid a bypass of the valves. The functions in (2) and (3) are given by a expression for mass flow rate through an orifice of constant area, which depends only on the upstream and downstream pressures [15]:

$$q_m(P_{up},P_{down}) = \begin{cases} CP_{up}\sqrt{\dfrac{T_{atm}}{T_{up}}} \text{ if } \dfrac{P_{down}}{P_{up}} \le C_r \text{ (sonic)} \\ CP_{up}\sqrt{\dfrac{T_{atm}}{T_{up}}}\sqrt{1-\left(\dfrac{\frac{P_{down}}{P_{up}}-C_r}{1-C_r}\right)^2} \text{ otherwise (subsonic)} \end{cases} \quad (4)$$

where C_r is the critical pressure ratio and C is the sonic conductance; P_{up} and P_{down} are respectively the absolute upstream and downstream stagnation pressures of the valve (Pa); T_{atm} is the atmosphere temperature, and T_{up} is the upstream stagnation temperature.

III. CONTROL DESIGN

A. Hybrid control of a single pneumatic manipulator

1) Hybrid control principle

Hybrid control uses a hybrid model where the continuous state variables of the continuous system depend on the configuration of the energy modulator:

$$\dot{\underline{X}}(t) = f\left(X(t),\ \underline{u}(t)\right) \quad (5)$$

with $\underline{X}=(x_1, x_2,\ldots, x_m)\in \mathrm{R}^m$ where x_i, $1\le i \le m$, are the state variables of the system. Here, f is the dynamic function governing the state-space model and $\underline{u}$ is a control vector that includes the N possible values corresponding to the N configurations of the energy modular

$$\underline{u} \in \left\{\underline{u}_1, \underline{u}_2, \ldots, \underline{u}_N\right\}_{N\ge 2} \quad (6)$$

For a small sampling period T, the model (5) can be approximated by a discrete model using Euler's method:

$$\underline{X}\left((k+1)T\right) \approx \underline{X}(kT) + f\left(\underline{X}(kT), \underline{u}(kT)\right).T \quad (7)$$

The full state $\underline{X}(kT)$ is assumed to be measured at time kT. The state at time $(k+1)T$, denoted $\underline{X}_j((k+1)T)$, for each value of the configuration j, $1\le j \le N$, can be calculated by (7).
The N directions $\underline{d}_j$ in the state space are defined as

$$\underline{d}_j = \underline{X}_j\left((k+1)T\right) - \underline{X}(kT) \quad (8)$$

For a given reference state $\underline{X}_{ref}$ the hybrid control calculates the N possible directions $\underline{d}_j$. Thereby an optimal control

among the N configuration is chosen in order to track this reference in the state space.

For the two-dimensional example shown in Fig. 2, the desired value (target point) can be placed in the plane of x_1 and x_2. To track the reference signal at each sample time, the hybrid control algorithm proceeds as follows:

- Acquisition of the state variables at time kT: $x_1(kT)$ and $x_2(kT)$.

- Based on the state knowledge at time kT, an estimation of the state at time $(k+1)T$ is carried out based on (7). Because the control signal $\underline{u}$ belongs to a finite set of possibilities as assumed in (6), this step is equivalent to the calculation of the different directions $\underline{d}_j$, corresponding to the jth configuration of the energy modulator ($\underline{d}_1$ to $\underline{d}_5$ in Fig. 2).

- Knowing the target point at time kT, the algorithm selects the best possible configuration among the N configurations. The chosen configuration is the solution that minimizes the Euclidean distance between the different reachable points and the target point. For instance, the shortest Euclidean distance corresponding to $\underline{d}_4$ is chosen in the example of Fig. 2 and, therefore, the corresponding control u_4 is applied to the energy modulator.

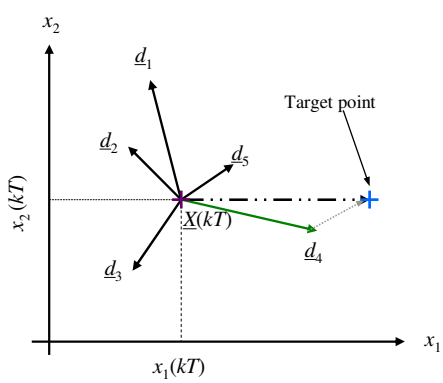

Fig. 2. Principle of hybrid control

2) Application to a pneumatic system

Because the control signals of the master and slave manipulators in a teleoperation system are force signals [17], the hybrid algorithm presented in Section III.A.1 is applied to a force tracking problem. The bilateral control of the teleoperation system will be detailed in section III.B.

For the system of Fig. 1 and the force tracking problem, the pressures in chambers p and n can form the state vector $X(t)=(P_n\ P_p)^T$. Each valve may show three different behaviors (pressure admission, closed, and pressure exhaust), leading to nine different control vectors u_1 to u_9, as shown in Table I.

TABLE I
NINE DISCRETE POSSIBLE STATES OF CONTROL

	$\underline{u}_1$	$\underline{u}_2$	$\underline{u}_3$	$\underline{u}_4$	$\underline{u}_5$	$\underline{u}_6$	$\underline{u}_7$	$\underline{u}_8$	$\underline{u}_9$
U_1	0	1	0	0	0	1	0	0	1
U_2	0	0	1	0	0	0	1	1	0
U_3	0	0	0	1	0	1	0	1	0
U_4	0	0	0	0	1	0	1	0	1

The objective, knowing the pressure at the sample time kT, is to estimate the evolution of the pressures at the next sample time $(k+1)T$ in chambers p and n for the nine controls (Table I), and then choose the best control for reaching the desired force. Assuming the variation of the pressures during a sampling time is small, the derivatives of the pressure can be rewritten as discrete expressions

$$\begin{cases} P_p\left((k+1)T\right) \approx \dfrac{d}{dt}\left(P_p(t)\right)\Big|_{t=kT} \times T + P_p(kT) \\ P_n\left((k+1)T\right) \approx \dfrac{d}{dt}\left(P_n(t)\right)\Big|_{t=kT} \times T + P_n(kT) \end{cases} \tag{9}$$

where the derivatives of the pressures are calculated based on (1)-(4). The expressions dP_p/dt and dP_n/dt are functions of P_p, P_n, y and v. At each sample time, P_p, P_n and y are measured by sensors, while v is estimated by numerical derivation of the position measurement y. Thus, for each of the nine control vectors, the algorithm calculates $P_p((k+1)T)$ and $P_n((k+1)T)$ based on (9). Consequently, the nine directions $\underline{d}_1$ to $\underline{d}_9$ define the set of reachable points at time $(k+1)T$ in the state space [16].

B. Bilateral 4-channel control of a pneumatic master-slave teleoperation system

Figure 3 depicts the general 4CH bilateral teleoperation architecture proposed by Lawrence [18].

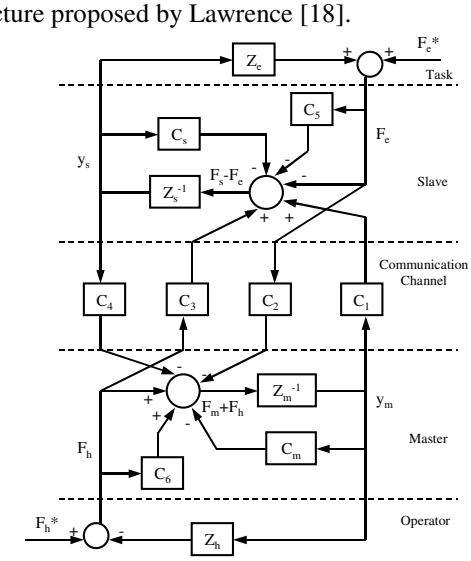

Fig. 3. 4CH bilateral control architecture

In this figure, impedances Z_h and Z_e denote the dynamic characteristics of the human operator's hand and the environment, respectively; Z_m and Z_s denote the master and slave manipulators' linearized dynamics, which are generally approximated by simple mass-spring-damper systems; F_h and F_e are the operator force exerted on the master and the environment force exerted on the slave; F_m and F_s are the (force) control signals for the master and slave manipulators; y_m and y_s are the master and slave positions; C_m and C_s denote the local position controllers of the master and the slave

sides; C_5 and C_6 are local force feedback terms for the master and the slave; and C_1 to C_4 are position or force controllers embedded in the communication channel. Also, F_h^* and F_e^* are the operator's and the environment's exogenous input forces, respectively, and are independent of teleoperation system behavior. It is generally assumed that the environment is passive ($F_e^*=0$) and the operator is passive in the sense that he/she does not perform actions that will make the teleoperation system unstable.

The architecture in Fig. 3 involves four types of data transmission between the master and the slave: force and position (or velocity) from the master to the slave and vice versa. It is shown in [18] that having these four channels of data transmission is of critical importance in achieving high-performance telepresence (i.e., full transparency) in terms of accurate transmission of task-related information such as the environment impedance to operator. Nonetheless, by proper adjustment of the local feedback parameters (C_5 and C_6), it is possible to obtain two classes of three-channel architectures, which can perform as well as the 4CH system [19]. We assume that communication time delay between the master and the slave is negligible.

The dynamics of the master and slave robots can be written as

$$F_m + F_h = Z_m y_m \quad , \quad F_s - F_e = Z_s y_s \tag{10}$$

and the dynamics of the operator and the environment are

$$F_h = -Z_h y_m + F_h^* \quad , \quad F_e = Z_e y_s + F_e^* \tag{11}$$

Note that we have used positions in the above instead of velocities as shown in Lawrence's architecture [18]. This is due to the fact that ensuring velocity tracking between the master and the slave might cause small offsets between the master and slave positions (i.e., steady-state errors in position tracking). Generally, when the delay in the communication channel is negligible, the use of position controllers or velocity controllers does not affect the stability of the teleoperation system [18], thus we opt to use position controllers.

In an ideally transparent (high-performance) teleoperation system, the master and the slave positions and forces will match regardless of the operator and environment dynamics:

$$y_m = y_s \quad , \quad F_h = F_e \tag{12}$$

This will ensure that the teleoperation system displays undistorted dynamics of the environment to the operator. In the 4CH system of Fig. 3, perfect transparent teleoperation can be achieved if and only if the controllers satisfy the following conditions [19]:

$$C_1 = C_s + Z_s, C_4 = -(C_m + Z_m), C_6 + 1 = C_2, C_5 + 1 = C_3 \tag{13}$$

Applying (13) to Fig. 3 yields

$$\begin{cases} C_2(F_h - F_e) = (Z_m + C_m)(y_m - y_s) \\ C_3(F_h - F_e) = (-Z_s - C_s)(y_m - y_s) \end{cases} \tag{14}$$

On the other hand, as discussed before, the master and slave dynamics Z_m and Z_s can generally be modeled by simple mass-spring-damper systems. As it is evident from the closed-loop equations (14) for the master and the slave, if the master and slave dynamics include damping terms, they contribute to the closed-loop equations in the same way as the derivative terms of the master and slave PD controllers (i.e., C_m and C_s). Similarly, the spring stiffness terms in the master and slave dynamics can be combined with the proportional terms in C_m and C_s. Therefore, in most of the teleoperation literature, Z_m and Z_s are considered to be pure inertias.

The control laws described in (13) for C_1 and C_4 require acceleration measurements (due to the inertial contributions of Z_m and Z_s). If a good transparency is required over a large frequency bandwidth, accurate estimation of inertial parameters based on accelerometers may be justified [20]. However, at low frequencies, near-transparency can be obtained by ignoring the master and slave dynamics in the expressions for C_1 and C_4 [21], in which case the original control design (13) is modified to

$$C_1 = C_s, \quad C_4 = -C_m, \quad C_6 + 1 = C_2, \quad C_5 + 1 = C_3 \tag{15}$$

With the choice of controllers in (15), based on Fig. 3 the master and slave closed-loop equations become

$$\begin{cases} C_2(F_h - F_e) = Z_m y_m + C_m(y_m - y_s) \\ C_3(F_h - F_e) = Z_s y_s - C_s(y_m - y_s) \end{cases} \tag{16}$$

There is more than one way to choose the controllers in (15). Normally, the position controllers are chosen such that $C_m/C_s = Z_m/Z_s$ to achieve similar closed-loop dynamics for the master and the slave [22]. Since in our experiments the master and the slave robots are identical $Z_m = Z_s = Z$, we take their controllers to be similar as well:

$$C_s = C_m = C_p \quad , \quad C_2 = C_3 = C_f \tag{17}$$

where C_p and C_f are the position and force controllers to be determined. . Normally, C_p is a PD-type controller and C_f is a scalar gain. With the choice of controllers in (17) and based on the closed-loop equations (16) and, the position error dynamics becomes

$$(Z + 2C_p)(y_m - y_s) = 0 \tag{18}$$

indicating that the slave and master positions track each other asymptotically. A complete discussion of this point using the hybrid matrix analysis can be found in [22].

With perfect position tracking, (16) can be rewritten as

$$C_f(F_h - F_e) = Zy_m = Zy_s \tag{19}$$

Therefore, force tracking is not perfect for a high magnitude of Z (i.e., for high inertia or high frequencies). Had we used the acceleration measurements needed in (13), the force tracking error would have converged to zero – a fact corroborated by (14). It is also intuitively clear that lack of knowledge about the manipulator's dynamics in (15) can deteriorate the force tracking performance especially over high frequencies. However, for low frequencies, the right-hand side of (16) can be assumed to be negligible. Thus, from (16), F_h–F_e converges to zero. A good transparency can therefore be achieved at a low bandwidth. Worthy of note is

that since voluntary motions of the human hand are themselves band-limited, force tracking will be very good short of feeling high-frequency phenomena such as the sharp edges or texture of an object.

Thanks to the transparency conditions (15) and the simplifying assumption (17), the bilateral architecture in Fig. 3 with eight controller parameters (C_1 to C_6 , C_m and C_s) can be simplified to only two controller parameters (C_p and C_f), as shown in Fig. 4.

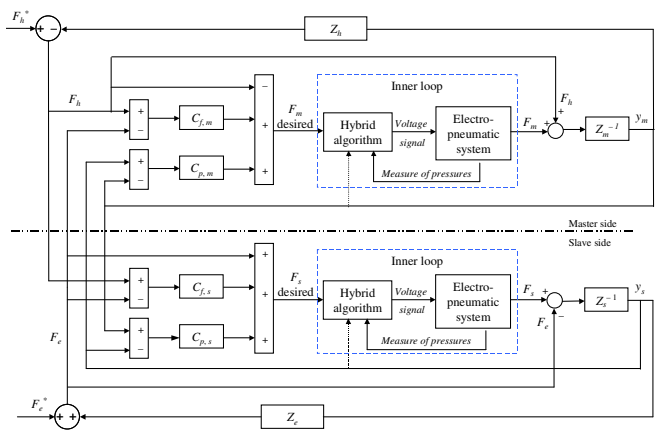

Fig. 4. 4CH bilateral teleoperation block diagram with hybrid control

A main difference between the original diagram in Fig. 3 and the diagram presented in Fig. 4 is that the hybrid algorithm is introduced. The input signals F_m+F_h and F_s–F_e correspond to the desired force of the hybrid control loop. If the force tracking obtained with the hybrid control is perfect, that means the behavior of the inner loop is equivalent to a unitary transfer function. Thus the diagram Fig. 3 is equivalent to the standard diagram Fig. 3. Thereafter the hybrid control loop is considered to be perfect to simplify the parameter controller calculations. The assumption will be verified in experiment in section V.

IV. Experimental Results and Discussion

A. Experimental setup

In this section, experiments are conducted with a one degree of freedom teleoperation system. The system setup consists of two identical devices (master and slave), actuated by two pneumatic cylinders using eight solenoid valves. The low friction cylinders (Airpel model M16D100D) have a 16 mm diameter and a 100 mm stroke. The end-effector of each manipulator is equipped with a force sensor in order to measure the operator's and the environment's forces. The pneumatic solenoid valves (Matrix model GNK821213C3) used to control the air flow have switching times of approximately 1.3ms (opening) and 0.2 ms (closing). With such fast switching times, the on/off valves are perfect for the purposes of the proposed control. The valve flow rate characteristics (4) used in the control scheme of Fig. 4 come directly from the data sheet of the components. A low-friction LVDT (Linear Variable Differential Transformer) position sensor is connected to each cylinder in order to measure the master's and the slave's positions. Each cylinder chamber is equipped with a pressure sensor. The system was supplied with air at an absolute pressure of 300 kPa.

The control system is implemented using a dSPACE board (DS1104), running at a sampling rate of 500 Hz. This value has been chosen according to the bandwidth of the valves and to guarantee acceptable tracking response.

B. Experimental results

Figure 5(a) gives the force tracking response and Fig. 5(b) presents the position tracking response obtained in the experiments. For the first few seconds, the master is moved back and forth by the user whereas the slave is in free space. It can be seen that the slave rapidly tracks the master's movement in free space. Next, the slave makes contact with a rigid environment. The operator pushes against the master leading to different levels of the slave/environment contact forces. The fact that the position profiles remain constant during the contact mode is that under hard contact the slave cannot penetrate the environment regardless of the operator's force.

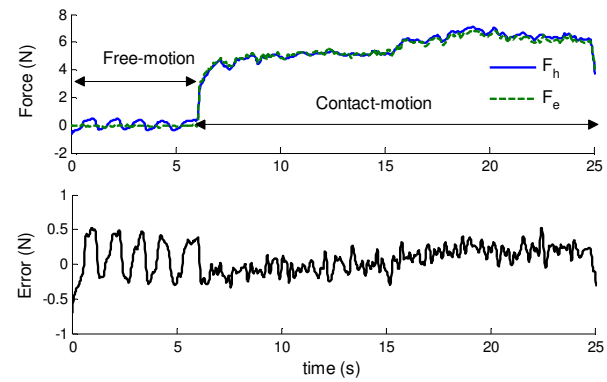

(a). Force tracking

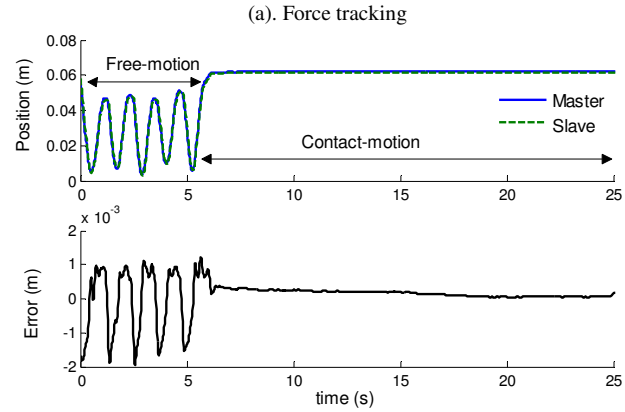

(b). Position tracking

Fig. 5. Experimental results of the master-slave system

Thanks to the force information, the operator can feel the slave/environment interaction in real time. Moreover, he/she can accurately transmit his/her force to the slave manipulator in order to perform a task. Note that the fast movements of

the master in the first few seconds do not present oscillations, but are intentionally created by the operator to examine the system stability and the performance in free motion. The nonzero values for F_h, even when the slave is in free space, is mainly due to the uncompensated friction of the pneumatic actuator. The experimental results show a good position and force tracking performance in free motion and under hard contact.

As mentioned in Section III.B, the transparency in Fig. 4 can be achieved when the inner force control loop is perfect. This condition is verified in Fig. 6, where the force generated by the slave actuator accurately tracks the desired force F_s. A similar result can be observed for the master system. The experimental results highlight that good performances for the force tracking of the inner closed-loop are obtained within the bandwidth of the movement. In our experimental validation, the movements were slow enough to assume that the pressure variation is small. The approximation (9) is entirely justified in this case. For faster movements, the tracking performances decrease but this drawback can be overcome by choosing a smaller sample time.

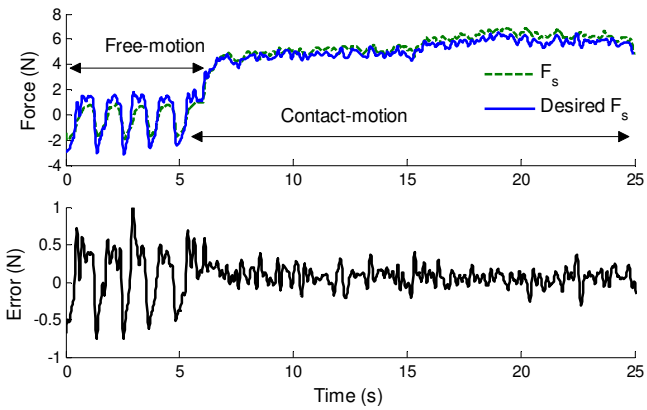

Fig. 6. Performance of the inner force control loop

V. Conclusion

In this paper, pneumatic actuators with inexpensive solenoid valves are chosen for the development of a master and slave teleoperation system. To control efficiently the switching on/off valves, a new hybrid algorithm has been successfully implemented in experiments. This technique not only takes into account the non-linear behavior of the mass flow rate but also the switching control of the solenoid valves. The results show that it is possible to achieve an acceptable transparent teleoperation performance without using classical proportional servovalves. With a four-channel bilateral architecture, under free-motion condition or contact-motion condition, the force and position tracking obtained is satisfactory. Lastly, future works consist of implementing the bilateral control with the hybrid algorithm on a multiple degree of freedom master/slave system. Another aspect of this work is the stability study of the hybrid control based teleoperation system, e.g., with respect to parameter uncertainties in the models.

References

[1] H. Kazerooni, "Human-robot interaction via the transfer of power and information signals", *IEEE Trans. Sys. Man. & Cyber*, pp. 450-463, 1990.

[2] B. Hannaford, "Scaling, impedance, and power flows in force reflecting teleoperation", *Rob. Res. ASME DSC*, pp. 229-232, 1990.

[3] S.P. DiMaio, S.E. Salcudean, C. Reboulet, S. Tafazoli, K. Hashtrudi-Zaad, "A virtual excavator for controller development and evaluation", *IEEE Int. Conf. Rob. & Auto. ICRA*, pp. 52-58, 1998.

[4] C. Melchiorri, A. Eusebi, "Telemanipulation: System aspects and control issues", *Proc. Int. Summer school Modeling & Control of Mechanisms and Robots*, Eds. Singapore, World Scientific, pp. 149-183, 1996.

[5] D. Stokic, M. Vukobratovic, D. Hristic, "Implementation of force feedback in manipulation robot", *Int. J. Rob. Res.*, pp. 66-76, 1986.

[6] N. Chopra, M.W. Spong, R. Ortega, N.E. Barabanov, "Position and force tracking in bilateral teleoperation", *Advances in Communication Control Network*, pp. 269-280, 2004.

[7] K. Tadano, K. Kawashima, "Development of a master slave system with force sensing using pneumatic servo system for laparoscopic", *IEEE Int. Conf. Rob. & Auto.*, Vol. 18, No. 1, pp. 947-952, 2007.

[8] K. Durbha, P.Y. Li, "Passive bilateral tele-operation and human power amplification with pneumatic actuators", *ASME Proc. Dynamic Systems and Control*, USA, October 2009.

[9] M. Taghizadeh, A. Ghaffari, F. Najafi, "Improving dynamic performances of PWM-driven servo-pneumatic systems via a nouvel pneumatic circuit", *Elsivier ISA Trans.*, pp. 512–518, 2009.

[10] X. Shen, J. Zhang, E. J. Barth, and M. Goldfarb, "Nonlinear averaging applied to the control of pulse width modulated pneumatic systems," *Proc. Amer. Control*, vol. 5, pp. 4444–4448, 2004.

[11] T. Nguyen, J. Leavitt, F. Jabbari, J.E. Bobrow, "Accurate sliding-mode control of pneumatic systems using low-cost solenoid valves", *IEEE Trans. ASME*, vol. 12, No. 2, pp. 216–219, 2007.

[12] J.M. Retif, X.F.Lin-Shi, A. Llor, "A new hybrid direct-torque control for a winding rotor synchronous machine", *35th IEEE* PESC *Power Electronics Specialists Conference*, 2004.

[13] M.Q. Le, M.T. Pham, R. Moreau, T. Redarce, "Comparison of a PWM and a hybrid force control for a pneumatic actuator using on/off solenoid valves", *IEEE Int. Conf. AIM*, pp. 1146-1151, 2010.

[14] J.L. Shearer, "Study of pneumatic processes in the continuous control of motion with compressed air", *ASME Trans.,* pp. 233–249, 1956.

[15] D. McCloy, H.R. Martin, "Control of fluid power: Analysis and design", *Ellis Horwood*, 505 p. ,1980.

[16] M.Q. Le, M.T. Pham, R. Moreau, T. Redarce, "Transparency of a pneumatic teleoperation system using on/off solenoid valves", *IEEE Int. Conf. RoMan*, September, 2010, accepted paper.

[17] M. Tavakoli, R.V. Patel, M. Moallem, A. Aziminejad, "Haptics for teleoperated surgical robotic systems", *World Scientific Publishong Co. Pte. Ltd.*, ISBN-13 978-981-281-315-2, 2008.

[18] D.A. Lawrence, "Stability and transparency in bilateral teleoperation", *IEEE Trans. Rob. & Auto. 9*, pp. 624-637, 1993.

[19] K. Hashtrudi-Zaad, S.E. Salcudean, "Transparency in time-delayed systems and the effect of local force feedback for transparent teleoperation", *IEEE Rob. Auto.*, Vol. 18, No. 1, pp. 108-114, 2002.

[20] Y. Yokokohji, T. Yoshikawa, "Bilateral control of master-slave manipulators for ideal kinesthetic coupling-formulation and experiment", *IEEE Trans. Rob. & Auto. 10*, pp. 605-620, 1994.

[21] S.E. Salcudean, M. Zhu, W.H Zhu, K. Hashtrudi-Zaad, "Transparent bilateral teleoperation under position and rate control", *Int.Journal of Robotics Research*, Vol. 19, No. 12, pp.1185-1202, December 1998.

[22] M. Tavakoli, A. Aziminejad, R.V. Patel, M. Moallem, "High-fidelity bilateral teleoperation systems and the effect of multimodal haptics", *IEEE Trans. Sys., Man, Cybernetics*, Part B: Cybernetics, Vol. 37, No. 6, December 2007.